Tapered drip laterals and manifolds laid on flat fields: Analytical solutions and energy-saving potential

Giorgio Baiamonte, M.ASCE[1*], Samuel Palermo[2]

[1]Full Professor, Department of Agricultural, Food and Forest Sciences (SAAF), University of Palermo, viale delle Scienze, Bldg. 4, Palermo 90128, Italy. Corresponding Author. E-mail: giorgio.baiamonte@unipa.it

[2]PhD. Candidate, Department of Agricultural, Food and Forest Sciences (SAAF), University of Palermo, viale delle Scienze, Bldg. 4, Palermo 90128, Italy. E-mail: salvatoresamuel.palermo@unipa.it

Abstract

A new analytical procedure is developed to design microirrigation units of rectangular shape with tapered laterals and manifolds laid on flat fields. The methodology relies on a normalizing pressure heads approach based on the pressure head tolerances concept to assure limited emitter flow rate variability across all emitters. The results indicated that tapered laterals primarily enhance energy saving and efficiency in drip irrigation systems. Moreover, the proposed procedure included new relationships for tapered laterals and manifolds helping identify commercial characteristics of emitters and pipe diameters. The validation of the proposed analytical procedure was performed by the comparison of results with the precise stepwise solution conducted for #1000 simulations. Since the procedure had been based on the assumption of uniform emitter flow rates, no errors occurred when the exponent x of the emitter flow relation was set equal to zero. Whilst for non-pressure

compensating emitters ($x > 0$) slight relative errors in inlet pressure head, *RE*s, occur, laying in a very limited range, from −1.2 % to 0.8%, and reaching the maximum values for the fully laminar flow condition ($x = 1$). A numerical application was performed to illustrate the reliability of the suggested design procedure, also illustrating that an energy-saving *ES* = 55.6 % was achieved. Results also illustrated that much higher *ES*s can be achieved for different geometric and hydraulic characteristics of the tapered units. The proposed methodology could serve as a foundational framework for saving energy in drip irrigation systems, and for analyzing the effects of tapered laterals and manifolds on the design variables.

Keywords: Dual–diameter laterals; Energy–saving; Analytical solutions; trickle irrigation design

Introduction

Microirrigation systems, known for their water efficiency and precision, have become increasingly popular in addressing drought challenges, energy saving, and water losses (Madramootoo and Morrison 2013; Li 2020; Patel et al. 2023). Despite significant research on drip irrigation units, there is limited understanding of the use of tapered drip laterals and their design procedures. This work aims to suggest an analytical method to design drip irrigation units with tapered pipes, providing a comprehensive analysis of the principles, methodologies, and applications involved.

Tapered laterals and manifolds are characterized by a reduction in diameter along the pipeline in the direction of the flow. The use of tapered pipes makes the design process more complicated than single-diameter pipes, because of the increase in the number of variables, but results in a more uniform pressure head distribution, thereby ensuring consistent water emission uniformity across all emitters (Valiantzas 2003; Sadeghi and Peters 2012; Baiamonte 2018a; Baiamonte et al. 2024). The design and optimization of these systems require a robust analytical framework that considers various factors and parameters, including hydraulic principles and emitter characteristics (Ayars et al. 2023).

The methodologies applied in designing drip irrigation units frequently rely on numerical approaches, such as the stepwise method, characterized by trial-and-error iterations and time-consuming calculations (Bralts and Segerlind 1985; Kang and Nishiyama 1997; Jiang and Kang 2010; Wang and Chen 2020; Ravikumar 2023). Furthermore, the results yielded by such methods do not facilitate a comprehensive analysis of pressure heads, emitter characteristics and inside diameters behavior when dealing with tapered pipes. Indeed, the stepwise method provides specific solutions for particular scenarios, which limits its usefulness in understanding the broader principles. Thus, the numerical method can result in low-efficient design solutions that negatively affect crop yield, as well as water and energy efficiency.

Whilst numerical approaches have been widely used in designing drip irrigation units, analytical methods offer a key advantage in providing insight into the design problem and include complete analyses, thereby overcoming the drawbacks of numerical ones. Analytical procedures can provide explicit solutions, offering more efficient tools to explore the effect of the design parameters on water distribution uniformity and energy efficiency (Chamba et al. 2019; Baiamonte et al. 2024). Unlike numerical methods that require iterative calculations, analytical solutions yield the required inlet pressure head for fixed pressure variability and pipe diameters in a single step, facilitating systematic analysis of their interactions with water distribution uniformity.

Various analytical methods were also proposed to design tapered drip laterals (Sadeghi et al. 2016; Yildirim 2023), which may require high levels of sophistication, making them not user-friendly due to the high number of variables involved in the calculation of pressure heads.

In consideration of the above, analytical methods were implemented in software to facilitate the complex process of designing (Krishnan and Ravikumar 2002; Moreno et al. 2016; Baiamonte 2018b; Palau et al. 2019). Molina-Martínez and Ruiz-Canales (2009) assessed the drip irrigation lateral diameters with on-line emitters employing Pocket PC software. The results included a diagram featuring light-emitting diodes (LEDs) illustrating the available commercial diameters when varying emitter number, spacing, and flow rate. Valipour (2012) used the HydroCalc software to compare the

effectiveness of single and tapered pipes in adjusting pressure loss. The study demonstrated that tapered pipes were capable of adjusting pressure loss, whereas single manifolds were unable to achieve the desired pressure head. Palau et al. (2019) developed DIMSUB, a computer program designed as a decision support tool to study different hydraulic design alternatives characterized by various unit geometry. The authors evidenced that irregular geometries and different laterals and manifolds feeding points can be easily examined with DIMSUB to achieve accurate results.

Recently, Baiamonte et al. (2023) proposed a simplified procedure for designing dual-diameter laterals based on the concept of pressure head tolerances, and in line with the normalized pressure head distribution approach. The authors also conducted an experimental validation to demonstrate the reliability of this methodology (Baiamonte and Palermo 2024a).

The objective of this study is to develop a comprehensive theoretical foundation for designing rectangular irrigation units with tapered drip laterals and manifolds, thereby expanding the procedure introduced by Baiamonte and Palermo (2024a), which was valid for just one tapered lateral. The design incorporates branching pipe networks with multiple tapered laterals and a single tapered manifold, all configured for use on flat fields. Detailed analyses and evaluations to enhance energy efficiency, and case studies to validate the proposed method are also included.

Methodology

The sketch of a drip submain unit with tapered pipes is shown in **Fig. 1,** where laterals and a manifold with dual-diameter are illustrated. The figure also shows a qualitative behavior of the pressure head distribution (PHD) along the manifold and lateral, where the drop in pressure head corresponding to the change in diameter can be observed. The characteristic pressure heads along the manifold (inlet pressure head, h_{in}, pressure head at the manifold diameter change, h_M, at the distal end, $h_{M,min}$), and along the lateral, (maximum pressure head, h_{max}, at the lateral diameter change, h_n,

at the distal end, h_{min}) are also depicted. Note that at the conjunction of the lateral with the manifold, $h_{M,min} = h_{max}$, which is a crucial condition for further developments.

Pressure head tolerances are a crucial aspect of drip irrigation system design that ensures uniform water distribution and optimal system performance. These tolerances refer to the acceptable range of pressure head variations within different components of the irrigation system. In this context, three different tolerances can be distinguished: i) the pressure head tolerance of the lateral namely the allowable pressure variation between the maximum pressure head of the lateral and the minimum ($h_{max} - h_{min}$), ii) the manifold pressure head tolerance that refers to the acceptable pressure variation from the inlet pressure head to the minimum in the manifold ($h_{in} - h_{M,min}$), and iii) the unit pressure head tolerance that encompasses the overall pressure variation across the entire irrigation unit, from the inlet pressure head to the minimum in the lateral ($h_{in} - h_{min}$), representing the combined pressure head changes in both the manifold and laterals. These tolerances were defined in the section "Lateral, manifold and unit pressure head tolerances".

Design relationships for tapered drip laterals

The methodology previously suggested for one-lateral units (Baiamonte and Palermo, 2024a) is shortly summarized in the following. Note that minor losses, as additional fraction of kinetic head in the energy balance equation, are neglected, since it is necessary for extending the analytical procedure to rectangular units. However, these minor losses could be incorporated using the equivalent length method developed by Baiamonte (2020), which facilitates their calculation without affecting the derivation of the design procedure.

Fig. 2 shows a tapered drip lateral laid on a horizontal field. The downstream segment, denoted as sub-lateral *I*, exhibits a smaller diameter, $D_{L,I}$ (L), compared to that of the upstream segment, denoted as sub-lateral *II*, which has a diameter $D_{L,II}$ (L). Emitters *j*s are numbered from right to left, so that N_I and N_{II} are the number of emitters on sub-laterals *I* and *II* with lengths L_I (L) and L_{II} (L),

129 respectively. Note that the total lateral length $L_L = L_I + L_{II}$ (**Fig. 2**). Once the geometry is established,
130 the design procedure could be applied for two or more sub-laterals, but for a simplified description
131 of the procedure, only two sub-laterals are considered later.

132 A uniform emitter flow rate is assumed, denoted as q_n ($L^3\ T^{-1}$), whereas S_I (L) and S_{II} (L),
133 indicate the emitter spacing of sub-lateral *I* and *II* respectively, so that $L_L = N_I\ S_I + N_{II}\ S_{II}$ with $N = N_I$
134 $+ N_{II}$. For the sublateral *I* ($j < N_I$), by neglecting local losses, the energy balance equation can be
135 written:

136

137 $$h_j = h_{min} + K_{L,I}\ S_I\ H_{j-1}^{(-r)} \qquad \text{for } j \leq N_I \qquad (1)$$

138

139 where $H_{j-1}^{(r)} = \sum_{k=1}^{j-1} \frac{1}{k^r}\ /; j \in \mathbb{N}$ is the generalized harmonic number truncated at the emitter $j - 1$, of
140 order *r* (Abramowitz and Stegun 1972), $K_{L,I}$ is the energy gradient corresponding to q_n, and S_I is the
141 emitter spacing associated with the sub-lateral *I*. According to Blasius resistance equation the energy
142 gradient $K_{L,I}$, can be written as:

143

144 $$K_{L,I} = k\ \frac{q_n^r}{D_{L,I}^s} \qquad (2)$$

145

146 where *r*, *s* and *k* depends on the resistance equation (Nakayama and Bucks 1986; Keller and Bliesner
147 1990). For smooth walled Polyethylene Pipe, Blasius'sand Hazen-Williams's equations can be
148 considered:

149

150 $$k = \frac{10.675}{C^r} \qquad r = 1.852,\ s = 4.871 \qquad \text{Hazen-Williams} \qquad (3a)$$

151 $$k = \frac{0.316\ 2^{2.5}}{g\ \pi^{1.75}} \nu^{0.25} \qquad r = 1.75,\ s = 4.75 \qquad \text{Blasius} \qquad (3b)$$

152

Where C is smoothness factor, g is the acceleration of gravity, and $\nu = 1.008\ 10^{-6}\ m^2\ s^{-1}$ is the water's kinematic viscosity for a standard water temperature at 20° C. Note that while the Hazen-Williams equation with C = 135 is used here (Moghazi 1998), this procedure can also be applied to any other resistance formula.

Of course, for $j = N_I$, $h_j = h_n$, and Eq. (1) yields:

$$h_n = h_{min} + K_{L,I}\, S_I\, H_{N_I}^{(r)} \tag{4}$$

where h_n is the pressure head corresponding to the diameter change that also appears in the energy balance equation for the sub-lateral *II* ($j > N_I$):

$$h_j = h_n + K_{L,II}\, S_{II} \left(H_{j-1}^{(r)} - H_{N_I}^{(r)} \right) \qquad \text{for } N_I + 1 < j \leq N \tag{5}$$

where $K_{L,II}$ can be calculated by Eq. (2), if replacing $D_{L,I}$ with $D_{L,II}$.

Substituting Eq. (4) into Eq. (5) provides:

$$h_j = h_{min} + K_{L,I}\, S_I\, H_{N_I}^{(r)} + K_{L,II}\, S_{II} \left(H_{j-1}^{(r)} - H_{N_I}^{(r)} \right) \tag{6}$$

In line with the normalized pressure head distribution approach, dimensionless relationships are used in the following to consolidate the influence of emitter spacing, inside diameter, and emitter flow rate. As a result, it becomes significantly easier to interpret the effects of proportional changes in one variable on another. This advantage is particularly pronounced when dealing with tapered laterals, because of the high number of parameters that are involved.

Dividing both sides of Eqs. (4) and (6) by $K_{L,I}$ and S_I, the same equations can be rewritten:

$$h_{*n} = h_{*min} + H_{N_I}^{(r)} \quad (7)$$

$$h_{*j} = h_{*min} + H_{N_I}^{(r)} + \frac{K_{L,II}\, S_{II}}{K_{L,I}\, S_I}\left(H_{j-1}^{(r)} - H_{N_I}^{(r)}\right) \quad (8)$$

Importantly, by using Eq. (2) and rearranging, Eq. (8) can be further simplified as follows:

$$h_{*j} = h_{*min} + H_{N_I}^{(r)}\left(1 + \frac{D_{*L}^{S}}{S_*}\,\Psi_j\right) \qquad \text{for } N_I + 1 < j \leq N \quad (9)$$

where:

$$D_{*L}^{S} = \frac{K_{L,II}}{K_{L,I}} = \left(\frac{D_{L,I}}{D_{L,II}}\right)^{S} \quad (10)$$

$$S_* = \frac{S_I}{S_{II}} \quad (11)$$

$$\Psi_j = \frac{H_{j-1}^{(r)}}{H_{N_I}^{(r)}} - 1 \quad (12)$$

Eq. (9) shows that the pressure head at the emitter *j* of the sub-lateral *II*, normalized with respect to $K_{L,I}$ and S_I, depends on the h_{*min}, diameter ratio D_{*L}, emitter spacing ratio $S_* = S_I/S_{II}$, and Ψ_j parameter (Eq. 12). The latter is affected by the harmonic number of the sub-lateral *I* and that truncated at the emitter *j* belonging to the sub-lateral *II*. Of course, for $j = N$, $h_{*j} = h_{*max}$, and Eq. (9) yields:

$$h_{*max} = h_{*min} + H_{N_I}^{(r)}\left(1 + \frac{D_{*L}^{S}}{S_*}\,\Psi_L\right) \quad (13)$$

where Ψ_L can be derived by Eq. (12), if imposing in it $j - 1 = N$:

$$\Psi_L = \frac{H_N^{(r)}}{H_{N_I}^{(r)}} - 1 \quad (14)$$

The normalized average pressure heads, h_{*n} and h_{*max}, can be expressed as a function of the pressure head tolerance of the laterals, δ_L, respectively:

$$h_{*n} = \frac{h_{*min}}{(1-\delta_L)} \quad (15)$$

$$h_{*max} = h_{*n}\,(1+\delta_L) \quad (16)$$

Combining Eq. (15) and (16), yields:

$$h_{*max} = h_{*min}\ \frac{1+\delta_L}{1-\delta_L} \quad (17)$$

Substituting Eq. (17) into Eq. (13), provides:

$$h_{*min}\ \frac{(1+\delta_L)}{(1-\delta_L)} = h_{*min} + H_{N_I}^{(r)}\ \left(1 + \frac{D_{*L}^{S}}{S_*}\ \Psi_L\right) \quad (18)$$

that can be solved with respect to h_{*min}:

$$h_{*min} = \frac{h_{min}}{K_{L,I}\,S_I} = \frac{1-\delta_L}{2\,\delta_L} H_{N_I}^{(r)}\ \left(1 + \frac{D_{*L}^{S}}{S_*}\ \Psi_L\right) \quad (19)$$

Therefore, for a fixed pressure head tolerance δ_L and hydraulic parameters of the tapered lateral, Eq (19) makes it possible to calculate the normalized minimum pressure head, h_{*min}. Moreover, by using Eqs. (15 and 19), the normalized average pressure head can be rewritten as a function of the input variables:

$$h_{*n} = \frac{h_n}{K_{L,I}\, S_I} = \frac{1}{2\,\delta_L} H_{N_I}^{(r)} \left(1 + \frac{D_{*L}^{S}}{S_*}\, \Psi_L\right) \quad (20)$$

Determining the characteristics of the emitter

Although the design procedure is developed under a uniform emitter flow rate assumption, the procedure could be also applied for non-pressure compensating emitters, i.e. when the exponent *x* of the emitter flow rate – pressure head relationship is greater than zero, if low values of the pressure head tolerance are imposed (Baiamonte 2024).

In this context, where the mean flow rate of the tapered drip laterals is assumed "constant", the emitter characteristics (k_e and emitter exponent *x*) of the flow rate – pressure head relationship, can be determined from the average pressure head h_n.

$$k_e = \left(\frac{q_n}{h_n}\right)^x \quad (21)$$

Substituting Eq. (20) into Eq. (21), yields:

$$k_e = \left(\frac{q_n\, 2\,\delta_L}{K_{L,I}\, S_I\, H_{N_I}^{(r)} \left(1 + \frac{D_{*L}^{S}}{S_*}\, \Psi_L\right)}\right)^x \quad (22)$$

Given input variables and emitter exponent, *x*, Eq. (22) enables identifying the coefficient k_e of the commercial emitters, a key parameter for the design. This contrasts with numerical methods, which typically require trial-and-error to estimate the characteristics of the emitters. For example, with reference to the characteristics of cylindrical integrated in-line labyrinth emitters (TANDEM®) with double holes and turbulent flow provided by IRRITEC S.p.A., reported in **Table 1**, choosing

$D_{L,I}$ = 13.8 mm, $D_{L,II}$ = 17.25 mm (i.e., D_{*L} = 0.8), $S_I = S_{II}$ = 0.5 m (i.e., S_* = 1), x = 0.49, for N = 175, **Fig. 3a** plots the relationship between the coefficient k_e and the emitters' number N_I (Eq. 22), with the average emitter flow rate as a parameter. To establish the N_I value that matches the k_e to be selected, **Fig. 3a** also plots dashed lines indicating the commercial k_e = 0.56 and 0.8 L h^{-1} m^{-x} values (**Table 1**), whereas the black dot refers to the application that will be performed later.

For the same emitter flow rates considered in **Fig. 3a**, by using Eq. (19), **Fig. 3b** plots the minimum pressure head, h_{min}, versus N_I, showing that at increasing N_I, the minimum pressure head required for the unit also increases. A similar illustration could be performed for the average pressure head of the laterals, h_n, by using Eq. (20).

Comparison with single-diameter lateral

Tapered drip laterals reduce the required inlet pressure head, thus decreasing the energy costs of microirrigation systems. However, the design lengths of the pipeline segments with different diameters must be carefully determined. The energy saving obtained by using tapered laterals can be determined by comparing with single diameter laterals for any N_I, D_{*L}, and pressure head tolerance, δ. For single diameter laterals Baiamonte (2018a, see Eq. 23) found a simplified relationship to calculate the average pressure head, which is reported in the following:

$$\frac{2\,\delta\,h_n}{K\,S} = H_N^{(r)} \tag{23}$$

where S is the emitters spacing, which is assumed to be constant for single-diameter lateral.

Eq. (23) can also be rewritten by normalizing h_n with respect to $K\,S$:

$$h_{*n}^{one} = \frac{1}{2\,\delta_L^{one}}\,H_{N_{one}}^{(r)} \tag{24}$$

where N_{one} is the number of the emitter for the single-diameter lateral, h_{*n}^{one} is the average normalized pressure head for a single diameter lateral, and $H_{N_{one}}^{(r)}$ is the generalized harmonic number truncated at the emitter N_{one}.

Substituting Eq. (15), which is also valid for single diameter laterals, into Eq. (24), yields:

$$h_{*min}^{one} = \frac{1-\delta_L^{one}}{2\,\delta_L^{one}}\, H_{N_{one}}^{(r)} \tag{25}$$

Assuming $S = S_I = S_{II}$ ($S_* = 1$), $N_{one} = N$ (which for a fixed value of S means that the one-diameter lateral length $L_{one} = L$), and $\delta_L^{one} = \delta_L$, by using Eqs. (19) and (25), the ratio h_{*min}/h_{*min}^{one} can be derived:

$$\frac{h_{*min}}{h_{*min}^{one}} = \frac{\frac{1-\delta_L}{2\,\delta_L} H_{N_I}^{(r)} \left(1+D_{*L}^{S}\ \Psi_L\right)}{\frac{1-\delta_L^{one}}{2\,\delta_L^{one}} H_{N_{one}}^{(r)}} \tag{26}$$

By rearranging, Eq. (26) yields a simplified form:

$$\frac{h_{*min}}{h_{*min}^{one}} = \frac{h_{*max}}{h_{*max}^{one}} = \frac{1+D_{*L}^{S}\,\Psi_L}{1+\Psi_L} \tag{27}$$

Interestingly, Eq. (27) is not affected by the pressure head tolerance δ and the total number of emitters, and because of Eq. (17) also expresses the h_{*max}/h_{*max}^{one} , which can be considered as an energy saving factor, under the $S_* = 1$ condition.

Fig. 4a shows the h_{*max}/h_{*max}^{one} ratio versus N_I/N ratio, by varying D_{*L} values (Eq. 27). The figure shows that for a fixed N_I/N, at decreasing of D_{*L} the energy h_{*max}/h_{*max}^{one} decreases, improving the energy saving. For example, for N_I/N = 0.526 (black dot), which refers to the application that will

be performed later, for tapered laterals the required inlet pressure head is 45.2 % less than that of one-diameter laterals. Of course, all curves join in $N_I/N = 1$.

In conclusion, the benefit in terms of energy saving depends on the length of sub-lateral *II*, which has larger diameters than the sub-lateral *I*, as well as on the diameter ratio, D_{*L}. When the diameter of the upstream segment (the sub-lateral *II*) is larger than that of sub-lateral *I* (i.e. low D_{*L} values), the energy saving highly increases. On the other hand, the increase in pipe diameters determines an increase in the unit's costs.

From a practical point of view, only D_{*L} values ranging from 0.65 to 0.8 are commercially available, and for this D_{*L} range, the suggested procedure allows economic analysis to be performed that however is beyond the objective of this work.

Design relationships for tapered manifolds

A sketch of a tapered manifold with many dual-diameter laterals is displayed in **Fig. 5**. By maintaining the same notation of the tapered laterals, the downstream segment of the manifold, denoted as sub-manifold *I*, exhibits a smaller diameter, $D_{M,I}$ (L), compared to that of the upstream segment, denoted as sub-manifold *II*, which has a diameter $D_{M,II}$ (L). Laterals are numbered from the distal end of the manifold to the inlet, so that $N_{rows,I}$ and $N_{rows,II}$ are the number of laterals on sub-manifolds *I* and *II* with lengths $L_{M,I}$ (L) and $L_{M,II}$ (L), respectively (**Fig. 5**). Note that $L_M = L_{M,I} + L_{M,II} = N_{rows,I}\, S_{rows,I} + N_{rows,II}\, S_{rows,II}$ with $S_{rows,I}$ and $S_{rows,II}$ the drip lateral spacing of sub-manifold *I* and *II*.

Considering that the laterals along the manifold behave as emitters along the lateral (Palermo and Baiamonte 2023), the simplified relationships developed for tapered laterals can be easily extended to the manifold. According to the latter, replacing D_{*L} by D_{*M}, S_* by $S_{*rows} = S_{rows,I}/S_{rows,II}$, δ_L by δ_M, Ψ_L by Ψ_M, and $H_{N_I}^{(r)}$ by $H_{N_{rows,I}}^{(r)}$, Eq. (20) can be applied to the manifold to provide the relationship of the average pressure head of the manifold, h_M, normalized with respect to $K_{M,I}\, S_{rows}$, which is denoted as h_{*M}:

$$h_{*M} = \frac{h_M}{K_{M,I}\, S_{rows}} = \frac{1}{2\,\delta_M} H^{(r)}_{N_{rows,I}} \left(1 + \frac{D^S_{*M}}{S_{*rows}}\, \Psi_M\right) \tag{28}$$

where δ_M is the manifold pressure head tolerance, $H^{(r)}_{N_{rows,I}}$ is the generalized harmonic number truncated at the lateral $i = N_{rows,I}$, S_{*rows} is the ratio $S_{rows,I}/S_{rows,II}$, usually set equal to one, $D_{*M} = D_{M,I}/D_{M,II}$, and the Ψ_M parameter depends on the harmonic numbers of the N_{rows} laterals, and on the number of laterals in the sub-manifold I, $N_{rows,I}$:

$$\Psi_M = \frac{H^{(r)}_{N_{rows}}}{H^{(r)}_{N_{rows,I}}} - 1 \tag{29}$$

Of course, for the sub-manifold I, the energy gradient $K_{M,I}$ appearing in Eq. (28) needs to be associated with the lateral flow rate ($N\, q_n$) and inside diameter $D_{M,I}$:

$$K_{M,I} = k\, \frac{(N\, q_n)^r}{D^S_{M,I}} \tag{30}$$

Once the relationship of the average normalized pressure head of the manifold is known (Eq. 28), it is shown here that the inside manifold diameters to assure the imposed pressure head tolerance, δ, can be derived.

Indeed, using Eq. (30) to express the average normalized manifold pressure head, h_{*M}, provides:

$$h_{*M} = \frac{h_M}{K_{M,I}\, S_{rows}} = \frac{h_M}{S_{rows}}\, \frac{D^S_{M,I}}{k\,(N\, q_n)^r} \tag{31}$$

that can be solved with respect to the lateral flow rate, $N\, q_n$:

$$N\ q_n = \left(\frac{D_{M,I}^{s}\ h_M}{k\ S_{rows}\ h_{*M}}\right)^{1/r} \quad (32)$$

Repeating the same steps for the average normalized lateral pressure head (i.e. combining Eq. 2 and 20), h_{*n} can be expressed:

$$h_{*n} = \frac{h_n}{S_I}\frac{D_{L,I}^{s}}{k\ {q_n}^r} \quad (33)$$

that can be solved with respect to q_n, analogously to Eq. (31):

$$q_n = \left(\frac{D_{L,I}^{s}\ h_n}{k\ S_I\ h_{*n}}\right)^{1/r} \quad (34)$$

Substituting Eq. (34) into Eq. (32) provides:

$$N\ \left(\frac{D_{L,I}^{s}\ h_n}{k\ S_I\ h_{*n}}\right)^{1/r} = \left(\frac{D_{M,I}^{s}\ h_M}{k\ S_{rows}\ h_{*M}}\right)^{1/r} \quad (35)$$

that can be solved with respect to $D_{M,I}$:

$$D_{M,I} = D_{L,I}\left(\frac{N^r\ h_{*M}\ S_{rows}}{\Delta\ h_{*n}\ S_I}\right)^{1/s} \quad (36)$$

where, considering that $h_{M,min} = h_{max}$ (**Fig. 1**), Δ is expressed as follows:

$$\Delta = \frac{h_M}{h_n} = \frac{h_{max}}{h_n(1-\delta_M)} = \frac{1+\delta_L}{1-\delta_M} \quad (37)$$

Finally, Eq. (36) can be further simplified and rearranged by considering Eqs. (20 and 28):

$$D_{M,I} = D_{L,I}\, N^{r/s} \left[\frac{S_{rows}}{S_I}\, \frac{\delta_L}{\delta_M\, \Delta}\, \frac{H^{(r)}_{N_{rows,I}} \left(1+\frac{D^S_{*M}}{S_{*rows}}\, \Psi_M\right)}{H^{(r)}_{N_I}\left(1+\frac{D^S_{*L}}{S_*}\Psi_L\right)} \right]^{1/s} \tag{38}$$

It is interesting to observe that for fixed D_{*L} and D_{*M} ratios, the sub-manifold *I* inside diameter, $D_{M,I}$, is linearly related to $D_{L,I}$, and linked to the other geometric variables according to the exponents *r* and *s* of the resistance equation considered in the design.

To finalize the design procedure of the rectangular unit, the required inlet pressure head, h_{in}, also needs to be determined. For an arbitrarily set manifold pressure head tolerance, δ_M, considering Eq. (37), h_{in} can be expressed as:

$$h_{in} = \Delta\, h_n(1 + \delta_M) \; = h_M\, (1 + \delta_M) \tag{39}$$

It can be shown that the ratio between h_{*max} and h^{one}_{*max}, expressed by Eq. (27) also matches the ratio between the inlet pressure head of the tapered unit, h_{in} (Eq. 39), and that of the standard single-diameter drip irrigation systems, h^{one}_{in}. This is because, substituting h_n from Eq. (20), into Eq. (39) provides:

$$h_{in} = \Delta \frac{K_{L,I}\, S_I}{2\, \delta_L} H^{(r)}_{N_I} \left(1 + \frac{D^S_{*L}}{S_*}\, \Psi_L\right)(1 + \delta_M) \tag{40}$$

Noting that h^{one}_{in} can be derived by the same Eq. (40) putting D_{*L} =1, yields:

$$h^{one}_{in} = \Delta \frac{K_{L,I}\, S_I}{2\, \delta_L} H^{(r)}_{N_I} \left(1 + \frac{\Psi_L}{S_*}\right)\, (1 + \delta_M) \tag{41}$$

Therefore, the ratio h_{in}/h_{in}^{one} can be derived from Eqs. (40 and 41), giving:

$$\frac{h_{in}}{h_{in}^{one}} = \frac{1+\frac{D_{*L}^{S}}{S_*}\Psi_L}{1+\frac{\Psi_L}{S_*}} \quad (42)$$

that for $S_* = 1$ demonstrates that the results illustrated in **Fig. 4a** can also be extended to h_{in}/h_{in}^{one}, as reported in dimensionless terms in the ordinate label.

Eq. (42) can be used to calculate energy saving *ES*, also considering different emitter spacing in both single diameter and tapered laterals:

$$ES = \left|\frac{h_{in}}{h_{in}^{one}} - 1\right| = \frac{1-D_{*L}^{S}}{1+S_*/\Psi_L} \quad (43)$$

as illustrated in **Fig. 4b**, under the $S_* = 1$ condition. **Fig. 4b** also plots the *ES* (black dot) corresponding to the application that will be performed later.

Lateral, manifold and unit pressure head tolerances

The unit pressure head tolerance, δ, which is usually imposed to limit the pressure head variation within a specific range in the design, is defined as:

$$\delta = \frac{h_{in}-h_{min}}{h_{in}+h_{min}} \quad (44)$$

and can be analytically derived, if expressing the numerator and the denominator of Eq. (44):

$$h_{in} - h_{min} = h_M(1 + \delta_M) - h_n(1 - \delta_L) \quad (45)$$

$$h_{in} + h_{min} = 2\, h_{min} + h_M(1 + \delta_M) - h_n(1 + \delta_L) \quad (46)$$

Substituting Eqs. (45 and 46) into Eq. (44), using Eqs. (15 and 16) in dimensional terms and rearranging, the relationship between δ, and its two components δ_M and δ_L can be derived, respectively:

$$\delta = \frac{\delta_M + \delta_L}{1 + \delta_M \delta_L} \quad (47)$$

$$\delta_M = \frac{\delta - \delta_L}{1 - \delta_L \delta} \quad (48)$$

$$\delta_L = \frac{\delta - \delta_M}{1 - \delta_M \delta} \quad (49)$$

Of course, Eq. (48) can be used if δ_L is fixed and δ_M needs to be calculated, the vice versa for Eq. (49). Note that to derive design relationships, minor losses must be neglected. This is because the additive local loss term in Eq. (19 or 20) would otherwise prevent the derivation of Eq. (38).

Inlet pressure heads and sub-manifold diameters analysis

The manifold inside diameters (Eq. 38) and inlet pressure head (Eq. 39) are two common key parameters to assess the performance of drip irrigation systems. Both affect the hydraulic performance and the distribution uniformity of emitter flow rate. For tapered laterals and manifold, it is shown here the dependance of h_{in} and $D_{M,I}$ from N_I/N ratio and δ_M.

For example, for the tapered laterals, we refer to the same parameters considered in **Fig. 3**, and nominal emitter's flow rate q_n = 3 L/h (x = 0.49, k_e = 0.8 L h^{-1} m^{-x}). Whereas for the tapered manifold, we assume that the total length is L_M = 100 m with a spacing between the laterals $S_{rows,I} = S_{rows,II}$ = 2 m and that the number of the laterals for the two segments are $N_{rows,I}$ = 23 and $N_{rows,II}$ = 27.

Imposing $D_{*M} = D_{M,I}/ D_{M,II} = 0.8$, **Fig. 6a** plots the diameter of sub-manifold I, calculated by Eq. (38), versus N_I/N ratio and δ_M. The figure shows that for any N_I/N, $D_{M,I}$ decreases at increasing δ_M. The inlet pressure head, h_{in} (Eq. 39), which also needs to be considered, is plotted in **Fig. 6b** versus N_I/N ratio and δ_M. Contrarily to $D_{M,I}$, the figure shows that for any N_I/N, h_{in} increases at increasing δ_M.

The results illustrated in **Fig. 6** demonstrate that δ_M needs to be accurately chosen, when designing drip irrigation units with tapered pipes, according to the arbitrarily imposed input parameters. Indeed, high δ_M values determine small inside manifold diameters (**Fig. 6a**), thereby decreasing the investment costs. On the other hand, high δ_M values also determine a high inlet pressure head, increasing the operational costs (**Fig. 6b**). The vice versa occurs for low δ_M.

In consideration of the above, a further analysis was performed to isolate the effect of the manifold pressure head tolerance on inlet pressure heads and manifold inside diameters. This is because Eqs. (38 and 39) can be rewritten in dimensionless terms, making more general the results illustrated in **Fig. 6**.

Substituting δ_L relationship (Eq. 49) into Eq. (38), a dimensionless solution of the inside diameter of the sub-manifold *I*, $D_{*M,I}$, depending only on δ and δ_M, can be derived:

$$D_{*M,I} = \frac{D_{M,I}^{S} S_I \, H_{N_I}^{(r)}\left(1+\frac{D_{*L}^{S}}{S_*}\Psi_L\right)}{D_{L,I}^{S} \, N^r S_{rows,I} H_{N_{rows,I}}^{(r)}\left(1+\frac{D_{*M}^{S}}{S_{*rows}}\,\Psi_M\right)} = \frac{\delta-\delta_M}{\delta_M+\delta\,\delta_M} \tag{50}$$

Similarly, substituting Eq. (49) in Eq. (20) and then into Eq. (39), a dimensionless solution of the inlet pressure head, h_{*in}, which also depends on δ and δ_M only, can be derived:

$$h_{*in} = \frac{h_{in}}{K_{L,I}\, S_I \, H_{N_I}^{(r)}\left(1+\frac{D_{*L}^{S}}{S_*}\Psi_L\right)} = \frac{(1+\delta)(1+\delta_M)}{2\,(\delta-\delta_M)} \tag{51}$$

Fig. 7a and **Fig. 7b** show the variation of dimensionless manifold diameter and inlet pressure head versus δ_M, respectively. It is noteworthy that the results reported in **Fig. 7** are of general validity since are independent of the geometric and hydraulic parameters. Moreover, Eqs. (50 and 51) have a crucial role in the objective of this work when designing units with tapered pipes for an assigned δ, confirming that the arbitrarily set δ_M needs to be accurately chosen. Eqs. (50 and 51) could be relevant to perform an economic analysis to detect the most convenient δ_M to be selected, thereby optimizing both the operational and investment costs. However, this analysis, which should include the additional fitting costs that tapered laterals require, was not included in this study, since it is beyond the purpose of this work.

Finally, it is interesting to note that the dimensionless groups derived in Eqs. (50 and 51) match with those reported in Baiamonte and Palermo (2024b), where the same groups depending on pressure heads tolerances facilitated the design of trapezoidal drip irrigation units.

Error analysis

An error analysis was conducted to evaluate the accuracy of the proposed methodology by comparing the analytical solution with the results obtained by the step-by-step numerical method. The latter has the advantage of being applied for non-pressure compensating emitters, i.e. when the exponent x of the emitter flow relation is greater than zero, thus helping detect the errors in the suggested design procedure that was developed under the simplified assumption of uniform flow rate ($x = 0$).

A high number (# 1000) of simulations were performed for different random combinations of the input parameters, S_I, S_{II}, N_I, N, D_{*L}, $D_{L,I}$, q_n, $S_{rows,I}$, $S_{rows,II}$, $N_{rows,I}$, $N_{rows,II}$, and D_{*M}, as well as for different exponent x, of the emitter flow relation ($q_n = k_e\, h^x$).

Due to the wide number of the involved parameters $S_{rows,I}$ was set equal to $S_{rows,II}$, and δ was set equal to 10 %. These equal spacings do not limit the results of the error analysis that will be

performed, moreover, they are conditions usually set in practice. The latter is because $S_{rows,I} \neq S_{rows,II}$ could be of interest only when multiple crops are irrigated in the same unit, and δ = 10 % is a unit pressure head tolerance commonly assumed (Wu 1992; Baiamonte et al. 2024).

For each input parameter, **Table 2** reports the range of variability within which the variables were randomly sampled, indicating their considerable wideness that makes the error analysis general. Moreover, each set of # 1000 of random simulations was replicated for eleven different values of the exponent *x* (0-1) which may characterize the flow relation of commercial emitters.

The relative error in the inlet pressure head estimated by the analytical procedure, *RE*, was calculated as:

$$RE = \frac{h_{in,\,analyt} - h_{in,\,SBS}}{h_{in,\,SBS}} \tag{52}$$

where $h_{in,analyt}$ is the inlet pressure head calculated by the present methodology, and $h_{in,SBS}$ is the inlet pressure head obtained by the SBS procedure.

For different *x*, **Fig. 8a** illustrates the *RE* results, calculated by Eq. (52) with respect to that obtained by the exact SBS procedure, clearly showing that *RE* increases at increasing *x*, as could be expected. A better illustration of the error analysis results is illustrated in **Fig. 8b** where, for the same simulations, the *RE* cumulative frequency distributions are plotted.

Interestingly, for $x = 0$ a vertical line is obtained, indicating that no errors occur under the same assumption adopted in the suggested solution. Whereas as *x* increases, a range of increasing variability of *RE* can be observed. It is worth noting that the *RE* range is slight, confined from –0.6% to 0.4%, for the common $x = 0.5$ value, and a bit wider (from –1.2% to 0.8%), for the fully laminar flow condition of the emitters ($x = 1$).

In conclusion, the error analysis revealed that the suggested methodology is suitable to be applied for designing drip irrigation units with tapered pipes also considering non-pressure compensating emitters, and it is expected it will be used in practice.

Example of application

For the parameters already indicated in **Figs. 3** and **6**, a numerical application of the presented procedure is performed, and the corresponding pressure head distribution is determined by applying the SBS method. The unit pressure head tolerance was set δ = 10 %, whereas that of the lateral δ_L = 5 %, which means from Eq. (48) δ_M = 5.02 %.

The lateral length, L_L, can be easily derived by the emitter number and their spacing, giving $L_I = N_I\, S$ = 46 m, $L_{II} = N_{II}\, S$ = 41.5 m and $L_L = L_I + L_{II}$ = 87.5 m, whereas the manifold length, L_M, is equal to $L_M = S_{rows,I}\ N_{rows,I} + S_{rows,I}\ N_{rows,I} = 2 \times 23 + 2 \times 27 = 100$ m.

For an imposed D_{*M} = 0.8, the calculated diameters of both sub-manifolds are $D_{M,I}$ = 60.7 mm (Eq. 38) and $D_{M,II} = D_{M,I} / D_{*M}$ = 75.9 mm. The inlet pressure for the tapered laterals can be calculated by Eq. (39), resulting in h_{in} = 17.45 m.

Eq. (41) makes it possible to calculate the inlet pressure head associated with a standard single-diameter drip irrigation system, resulting in h_{in}^{one} = 39.30 m. Thus, tapered laterals allow energy to be saved, since $h_{in} = 0.44\ h_{in}^{one}$, as illustrated in **Fig. 4a**, and the associated *ES* (Eq. 43) is equal to 55.6 % (**Fig. 4b**). Of course, at decreasing N_I/N and D_{*L}, higher energy-saving is expected (**Fig. 4a**).

For an exponent of the emitter flow relation x = 0.49, **Fig. 9** shows the pressure head distribution (PHD) of the unit obtained by the SBS method, where the minimum pressure head is h_{min} = 14.27 m and the maximum pressure head is h_{in} = 17.40 m, providing the pressure head tolerance of the unit δ = 9.87 %, which slightly differs from the 10 % value imposed in the design. The relative error, *RE* (Eq. 52), in the inlet pressure head, is equal (17.45 – 17.40) / 17.40 = 0.27 %, as can be also observed

in **Fig. 8**, indicating a negligible overestimation, with respect to the exact h_{in} obtained by the SBS method.

Quantifying the energy-saving for different tapered irrigation units

To quantify the energy-saving for different irrigation units, the #1000 simulations performed in the error analysis section, and obtained by randomly varying the geometry and hydraulic parameters (**Table 2**), were considered. For each simulation, the energy-saving, *ES*, was calculated from Eq. (43), which also accounts for different emitter spacing in both single and dual-diameter laterals, in line with **Table 2**. The use of Eq. (43) makes homogeneous the comparison between tapered and single diameter laterals, since the total length of the laterals is the same in both cases, also for $S_I \neq S_{II}$.

For the #1000 simulations, **Fig. 10** shows the results of the energy-saving calculation, indicating that *ES* can achieve 88 %. Of course, the highest *ES* values correspond to low values of D_{*L}, S_*, and N_I/N (i.e., high Ψ_L, Eq.14), as can also be observed by Eq. (43).

Fig. 10 also plots the dot corresponding to the application illustrated in **Fig. 9**, for which *ES* = 55.6 % was found (**Fig. 4b**).

Conclusions

The following conclusions were drawn in this study:

1. Simplified relationships to design drip irrigation units with tapered laterals laid on flat fields were developed, under the assumption of uniform emitter flow rate (exponent *x* of the emitter flow relation equal to zero);
2. On the question of the tapered manifold inside diameters detecting, this study found an explicit relationship that depends on the geometric and hydraulic characteristics of the unit, for any pressure head tolerances of the laterals δ_L or of the manifold δ_M;

3. Given input variables, the proposed design procedure enables identifying the characteristics of the commercial emitters, thereby contrasting with numerical methods, which typically require trial-and-error.
4. The influence of tapered laterals and manifold pressure head tolerance δ_M, on inlet pressure head and manifold inside diameters was investigated;
5. An error analysis was performed by comparing the analytical solution with the step-by-step numerical one to evaluate the accuracy of the suggested procedure. Results showed that for $x = 0$, no relative errors in inlet pressure head estimation occurred. Whilst for emitter exponent $x = 1$, the maximum errors were obtained, laying in a negligible range (from –1.2% to 0.8%). For the most commonly used $x = 0.5$, the range of errors was even smaller (from –0.6% to 0.4%);
6. A numerical example to illustrate an application of the procedure suggested to design a rectangular unit with tapered laterals and manifold was performed, by considering non-pressure compensating emitters ($x > 0$). The pressure head tolerance of the unit resulted in $\delta = 9.87$ %, which slightly differs from the 10 % value imposed in the design, thus validating the methodology presented in this work.
7. Energy savings were evaluated by comparing the inlet pressure heads required by tapered and single-diameter laterals. Results indicated that energy savings remain fairly consistent regardless of the total lateral length. However, energy efficiency is significantly influenced by the fraction length of the small diameter segment and by the diameter ratio, D_{*L}. For #1000 simulations, obtained by randomly varying geometry and hydraulic parameters, it was shown that the energy-saving can achieve 88 %.

Notation

The following symbols are used in this paper:

592 C = smoothness factor of the Hazen-Williams resistance equation;

593 D_{*L} = the D_I/D_{II} ratio;

594 D_{*M} = the $D_{M,I}/D_{M,II}$ ratio;

595 $D_{*M,I}$ = normalized internal diameter of sub-manifold *I*;

596 $D_{L,I}$ = internal diameter of sub-lateral *I* [L];

597 $D_{L,II}$ = internal diameter of sub-lateral *II* [L];

598 $D_{M,I}$ = internal diameter of sub-manifold *I* [L];

599 $D_{M,II}$ = internal diameter of sub-manifold *II* [L];

600 ES = energy saving;

601 g = acceleration of gravity [L/T^2];

602 $H(.,.)$ = generalized harmonic number;

603 h_{*in} = normalized inlet pressure head;

604 h_{*j} = pressure head at the emitter *j* normalized with respect to S_I and $K_{L,I}$;

605 h_{*M} = pressure head at manifold diameter changing normalized with respect to $S_{rows,I}$ and $K_{M,I}$;

606 h_{*max} = maximum pressure head normalized with respect to S_I and $K_{L,I}$ for a tapered lateral;

607 h_{*min} = minimum pressure head normalized with respect to S_I and $K_{L,I}$ for a tapered lateral;

608 h_{*n} = pressure head at diameter changing of the lateral normalized with respect to S_I and $K_{L,I}$;

609 h_{in} = inlet pressure head [L];

610 $h_{in,analyt}$ = inlet pressure head calculated by the analytical procedure [L];

611 $h_{in,SBS}$ = inlet pressure head calculated by the numerical procedure [L];

612 h_j = pressure head at the emitter *j* [L];

613 h_M = pressure head at diameter changing of the manifold [L];

614 $h_{M,min}$ = minimum pressure head of the manifold [L];

615 h_{min} = minimum pressure head [L];

616 h_n = pressure head at diameter changing of the lateral [L];

617 h_{*max}^{one} = maximum pressure head normalized with respect to *S* and *K* for a single diameter lateral;

618 h_{*min}^{one} = minimum pressure head normalized with respect to *S* and *K* for a single diameter lateral;

619 h_{*min}^{one} = minimum pressure head normalized with respect to *S* and *K* for a single diameter lateral;

620 h_{*n}^{one} = average pressure head normalized with respect to *S* and *K* for a single diameter lateral;

621 h_{in}^{one} = inlet pressure head for a single diameter lateral [L];

622 i = generic lateral counted from the distal end of the manifold;

623 j = generic emitter counted from the distal end of the lateral;

624 k = flow resistance equation coefficient;

625 K = energy gradient for single diameter lateral;

626 k_e = coefficient in the emitter flow relation [V T^{-1} L^{-x}]

627 $K_{L,I}$ = energy gradient for sub-lateral *I*;

628 $K_{L,II}$ = energy gradient for sub-lateral *II*;

629 $K_{M,I}$ = energy gradient for sub-manifold *I*;

630 L_I = length of sub-lateral *I* [L];

631 L_{II} = length of sub-lateral *II* [L];

632 L_L = lateral length [L];

633 L_M = manifold lenght [L];

634 $L_{M,I}$ = length of sub-manifold *I* [L];

635 $L_{M,II}$ = length of sub-manifold *II* [L];

636 L_{one} = lateral length of a single diameter lateral [L];

637 N = total number of emitters of the lateral;

638 N_I = number of emitters on sub-lateral *I*;

639 N_{II} = number of emitters on sub-lateral *II*;

640 N_{one} = total number of emitters on a single diameter lateral;

641 N_{rows} = number of laterals on the manifold;

642 $N_{rows,I}$ = number of laterals on sub-manifold *I*;

643 $N_{rows,II}$ = number of laterals on sub-manifold *II*;

644 q_n = nominal (average) emitter flow rate [$L^3\ T^{-1}$];

645 r = flow rate exponent in the flow resistance formula;

646 s = diameter exponent in the flow resistance formula;

647 S = emitter spacing of single diameter laterals [L];

648 S_* = the $S_{rows,I}/S_{rows,II}$ ratio;

649 S_{*rows} = the S_I/S_{II} ratio;

650 S_I = emitter spacing of sub-lateral *I* [L];

651 S_{II} = emitter spacing of sub-lateral *II* [L];

652 $S_{rows,I}$ = lateral spacing of sub-manifold *I* [L];

653 $S_{rows,II}$ = lateral spacing of sub-manifold *II* [L];

654 x = emitter exponent

655 Ψ_j = ratio of the generalized harmonic numbers corresponding to a tapered lateral for the

656 emitter *j* of sub-lateral *II*;

657 Ψ_L = ratio of the generalized harmonic numbers corresponding to the tapered lateral;

658 Ψ_M = ratio of the generalized harmonic numbers corresponding to the manifold;

659 Δ = the h_M/h_N ratio;

660 δ = pressure head tolerance of the unit;

661 δ_L = pressure head tolerance for laterals;

662 δ_L^{one} = pressure head tolerance for single diameter laterals;

663 δ_M = pressure head tolerance for the manifold;and

664 ν = kinematic viscosity of water [$L^2\ T^{-1}$].

665

666 **Data Availability**

667

668 All data, models, and code generated or used during the study appear in the submitted article.

669

670 **References**

671

672 Abramowitz, M., and I. A. Stegun. 1972. *Handbook of mathematical functions*. New York: Dover
673 Publication.
674 Ayars, J. E., D. Zaccaria, and K. M. Bali. 2023. *Microirrigation for crop production: design,*
675 *operation, and management*. Elsevier Science.
676 Baiamonte, G. 2018a. "Advances in designing drip irrigation laterals." *Agr. Water Manage.* 199, 157–
677 174. https://doi.org/10.1016/j.agwat.2017.12.015.
678 Baiamonte, G. 2018b. "Explicit Relationships for Optimal Designing of Rectangular Microirrigation
679 Units on Uniform Slopes: the IRRILAB Software Application." *Comput. Electron. Agric.* 153,
680 151-168. https://doi.org/10.1016/ j.compag.2018.08.005.
681 Baiamonte, G. 2020. "Linking kinetic energy fraction and equivalent length method to determine
682 local losses in trickle irrigation." *J. Irrig. Drain. Eng.* 146 (8): 04020024.
683 https://doi.org/10.1061/(ASCE)IR.1943-4774.0001492.
684 Baiamonte, G. 2024. "Closed-Form solution of the length of drip laterals and easy selection of
685 commercial emitters for low-slope field under Hazen-Williams and Blasius resistance
686 equations." *Irrig. Drain. J.* 1-13. Doy*:* 10.1002/IRD.2969.
687 Baiamonte, G., M. Elfahl, and S. Palermo. 2023. "Experimental tests to validate a simple procedure
688 to design dual-diameter drip laterals on flat fields." In *12th International AIIA Conference AIIA*
689 *2022: Biosystems Engineering Towards the Green Deal. Improving the resilience of*
690 *agriculture, forestry and food systems in the post-Covid era*, 15-26. Palermo: Italian Society of
691 Agricultural Engineering.
692 Baiamonte, G., Palermo, S. 2024a. "Dual-diameter drip laterals laid on flat fields: modelling and
693 measurements." *Water Resour. Manag.* https://doi.org/10.1007/s11269-024-03976-9,
694 https://rdcu.be/dWCuK

695 Baiamonte, G., Palermo, S. 2024b. “Trapezoidal drip irrigation units laid on flat fields.” *J. Irrig.*
696 *Drain. Eng.*, Doi: 10.1061/JIDEDH/IRENG-10437
697 Baiamonte, G., Palermo, S., Sadeghi, S. H., and R. T. Peters. 2024. “Design Emission Uniformity of
698 Horizontal Tapered Drip Laterals from the Normalized Pressure Head Distribution Approach.”
699 *J. Irrig. Drain. Eng.* 150(4): 04024010. Doi: 10.1061/JIDEDH.IRENG-10300.
700 Bralts, V. F., and L. J. Segerlind. 1985. “Finite element analysis of drip irrigation submain units”.
701 *Trans. ASAE* 28(3): 809-814.
702 Chamba, D., S. Zubelzu, and L. Juana. 2019. “Energy, cost and uniformity in the design of drip
703 irrigation systems.” *Biosyst. Eng.* 178: 200-218.
704 Jiang, S., and Y. Kang. 2010. “Simple method for the design of microirrigation paired laterals.” *J.*
705 *Irrig. Drain. Eng.* 136(4): 271-275. https://doi.org/10.1061/(ASCE)IR.1943-4774.0000178.
706 Kang, Y., and S. Nishiyama. 1997. “An improved method for designing microirrigation submain
707 units.” *Irrig. Sci.* 17, 183-193.
708 Keller, J., and R.D. Bliesner. 1990. *Sprinkle and Trickle Irrigation*. New York: The Blackburn
709 Press.
710 Krishnan, M., and V. Ravikumar. 2002. “A software for design of drip subunits with tapered pipes in
711 non-uniform slopes.” *J. Agric. Eng.* 39 (4):28–36.
712 Li, J. 2020. “Microirrigation in China: History, current situation and future.” *Irrig. Drain. J.* 69: 88-
713 96. https://doi.org/10.1002/ird.2442.
714 Madramootoo, C. A., and J. Morrison. 2013. “Advances and Challenges with micro-irrigation.” *Irrig.*
715 *Drain.* 62: 255–261. https://doi.org/10.1002/ird.1704.
716 Moghazi HE-D M 1998. “Estimating Hazen-Williams coefficient for polyethylene pipes.” *J Transp*
717 *Eng* 124:197–199
718 Molina-Martínez, J. M., and A. Ruiz-Canales. 2009. “Pocket PC software to evaluate drip irrigation
719 lateral diameters with on-line emitters.” *Comput. Electron. Agric.* 69(1): 112-115.
720 http://dx.doi.org/10.1016/j.compag.2009.06.006.

721 Moreno, M.A., Del Castillo, A., Montero, J., Tarjuelo, J.M., and R. Ballesteros. 2016. “Optimisation
722 of the design of pressurised irrigation systems for irregular shaped plots.” *Biosyst. Eng.*, 151,
723 361-373. http://dx.doi.org/10.1016/j.biosystemseng.2016.10.005.
724 Nakayama, F. S., and D. A. Bucks. 1986. *Trickle Irrigation for Crop Production*. Amsterdam. The
725 Netherlands: Elsevier Science Publisher.
726 Palau, C. V., J. Arviza, I. Balbastre, and J. Manzano. 2019. “DIMSUB, a computer program for
727 designing microirrigation subunits. Tool definition and case studies.” *Sci. Agric.* 77,
728 e20180184.
729 Palermo, S., and G. Baiamonte. 2023. “Tapered drip laterals and manifolds in flat and rectangular
730 irrigation units.” In Vol. 17 of *Proc., EGU General Assembly Conf. Abstracts*, EGU-11522.
731 Gottingen, Germany: Copernicus Publications. https://doi.org/10.5194/egusphere-egu23-
732 11522.
733 Patel, A., N. L. Kushwaha, J. Rajput, and P. V. Gautam. 2023. “Advances in Micro-Irrigation
734 Practices for Improving Water Use Efficiency in Dryland Agriculture.” In Enhancing
735 Resilience of Dryland Agriculture Under Changing Climate: Interdisciplinary and Convergence
736 Approaches (pp. 157-176). Singapore: Springer Nature Singapore.
737 Ravikumar, V. 2022. *Design with telescopic pipes in uniform and non-uniform slopes*. Singapore:
738 Springer Nature Singapore.
739 Sadeghi, S. H., and T. Peters. 2012. “Analytical determination of distribution uniformity for
740 microirrigation tapered laterals laid on uphill and horizontal slopes.” *J. Irrig. Drain. Eng.* 139
741 (6): 483–489. https://doi .org/10.1061/(ASCE)IR.1943-4774.0000568.
742 Sadeghi, S. H., T. Peters, and V. Shelia. 2016. “Energy grade line assessment for tapered
743 microirrigation laterals.” *J. Irrig. Drain. Eng.* 142 (7): 04016020.
744 https://doi.org/10.1061/(ASCE)IR.1943-4774.0001020.

745 Valiantzas, J. D. 2003. “Explicit hydraulic design of microirrigation submain units with tapered
746 manifold and laterals.” *J. Irrig. Drain. Eng.* 129(4), 227-236.
747 https://doi.org/10.1061/(ASCE)0733-9437(2003)129:4(227).
748 Valipour, M. 2012. “Sprinkle and trickle irrigation system design using tapered pipes for pressure
749 loss adjusting.” *J. Agric. Sci.* 4(12): 125-133. http://dx.doi.org/10.5539/jas.v4n12p125.
750 Wang, J., and R. Chen. 2020. “An improved finite element model for the hydraulic analysis of drip
751 irrigation subunits considering local emitter head loss.” *Irrig. Sci.* 38 (2): 147–162.
752 https://doi.org/10.1007/s00271-019-00656-0.
753 Wu, I.P. 1992. “Energy gradient line approach for direct hydraulic calculation in drip irrigation
754 design.” *Irrig. Sci.*, 13:21-29. https://doi.org/10.1007/BF00190241.
755 Yıldırım, G. 2023. *Hydraulic Principles and Design Concepts for Submain Units with Multiple Outlet*
756 *Pipelines: New Analytical Techniques with Engineering Applications*. Cham: Springer
757 International Publishing.

Table 1 – Characteristics of the cylindrical integrated in-line labyrinth emitters (TANDEM®) with double holes and turbulent flow, provided by IRRITEC S.p.A. (emitters spacing, S, nominal diameter, ϕ, inside diameter, D, and emitter parameters, k_e and x).

S (m)	ϕ (mm)	D (mm)	k_e (L h^{-1} m^{-x})	x	emitter color
0.2	16	13.8	0.43	0.55	yellow
0.3			0.69	0.50	blue
0.4			1.32	0.49	black
0.5			2.48	0.51	red
0.6	20	17.25	0.56	0.52	yellow
0.75			0.80	0.49	blue
1			1.2	0.48	black
1.25			2.35	0.49	red
1.5			4.94	0.47	green

Table 2 – Ranges of the design variables selected to perform the #1000 random simulations.

	S_I, S_{II} (m)	N_I	N	δ_L	D_{*L}	$D_{L,I}$ (mm)	q_n (L h^{-1})	$S_{rows,I} = S_{rows,II}$ (m)	$N_{rows,I}$	N_{rows}	D_{*M}	δ
min	0.5	20	50	0.01	0.65	13.8	2	1	20	50	0.65	0.1
max	1.5	N	300	0.05	0.80	17.7	8	4	N_{rows}	150	0.80	

Figure_1

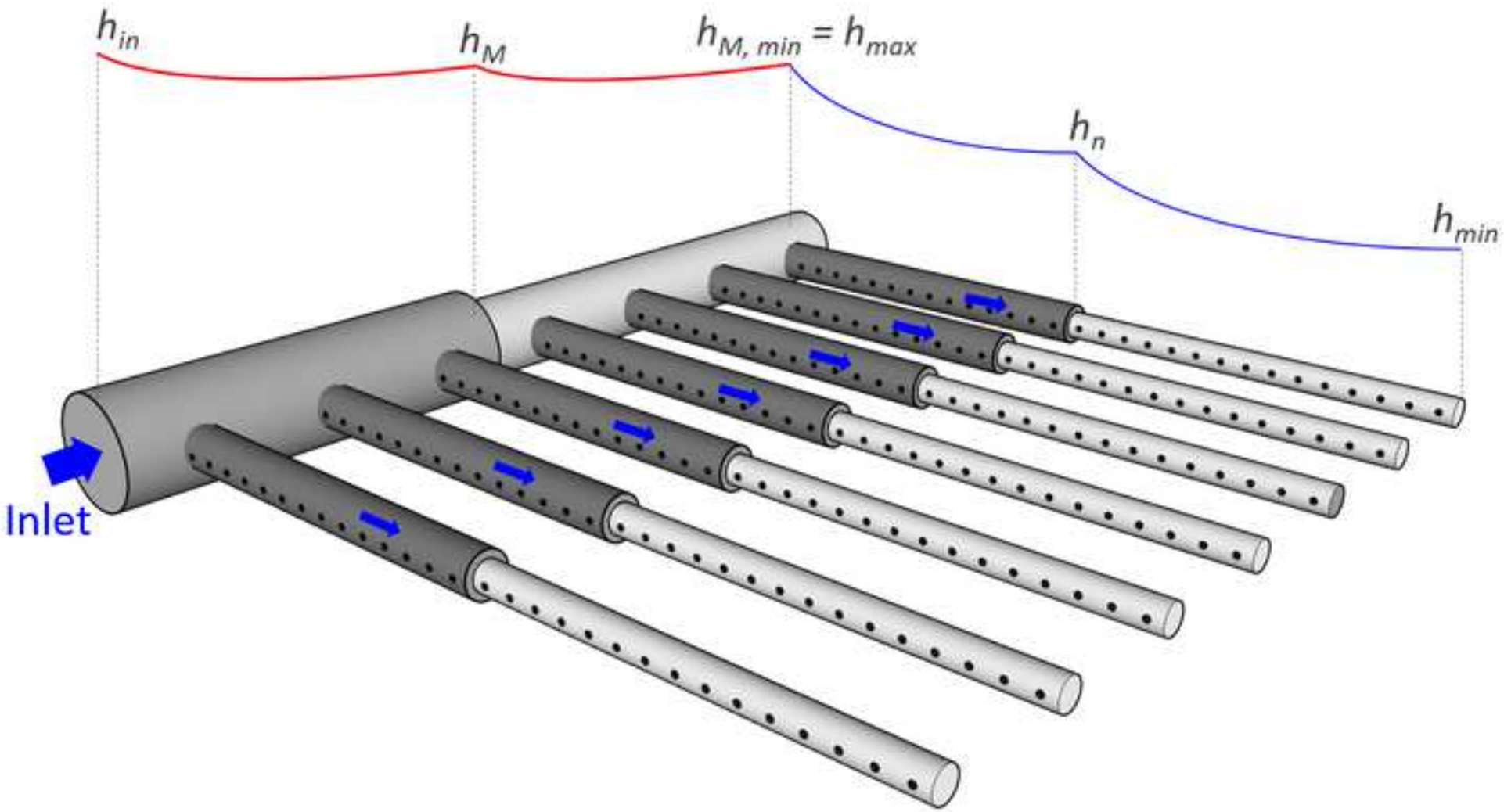

Figure_2

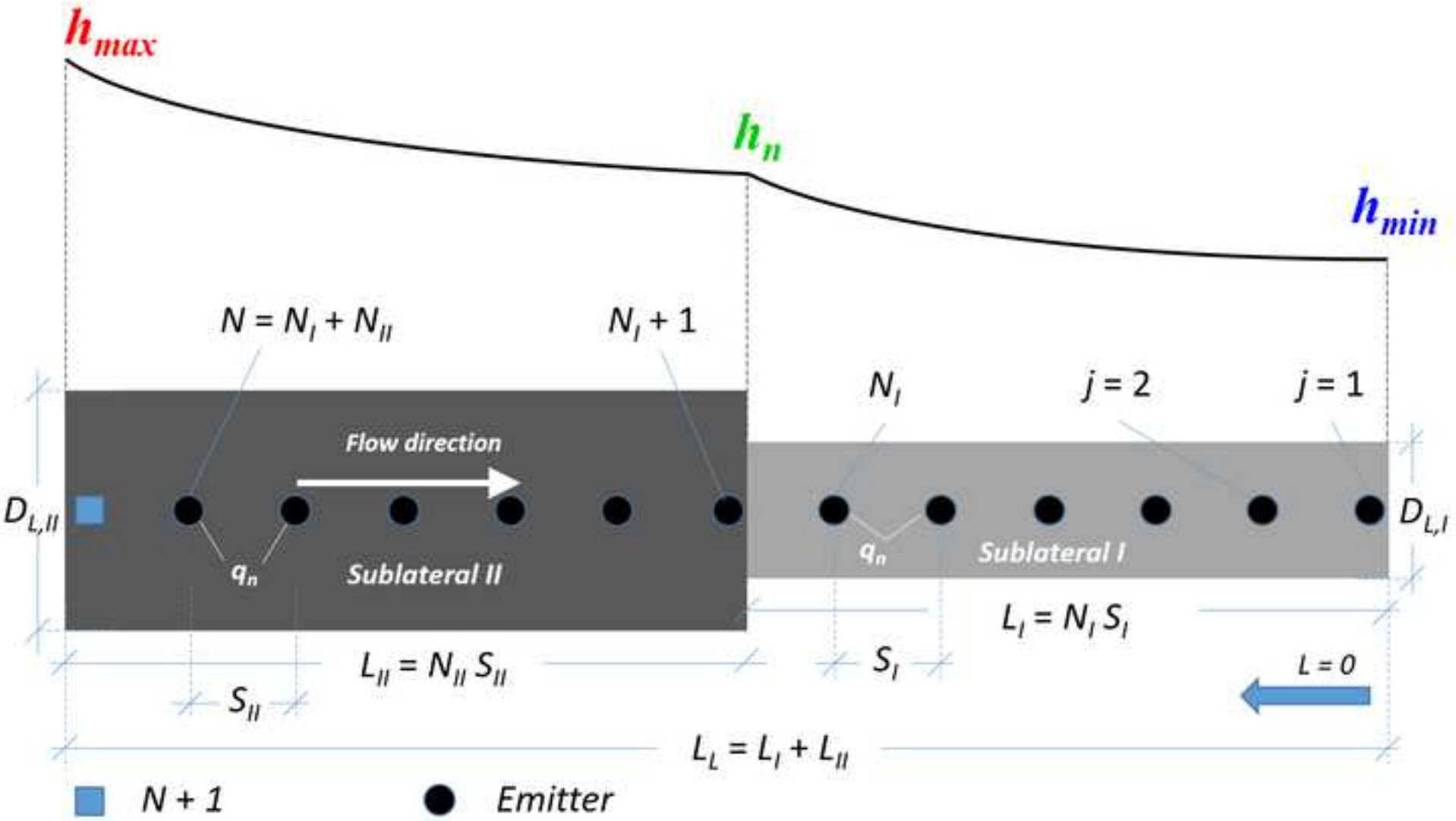

Figure_3

Click here to access/download;Figure;Figure_3.tif

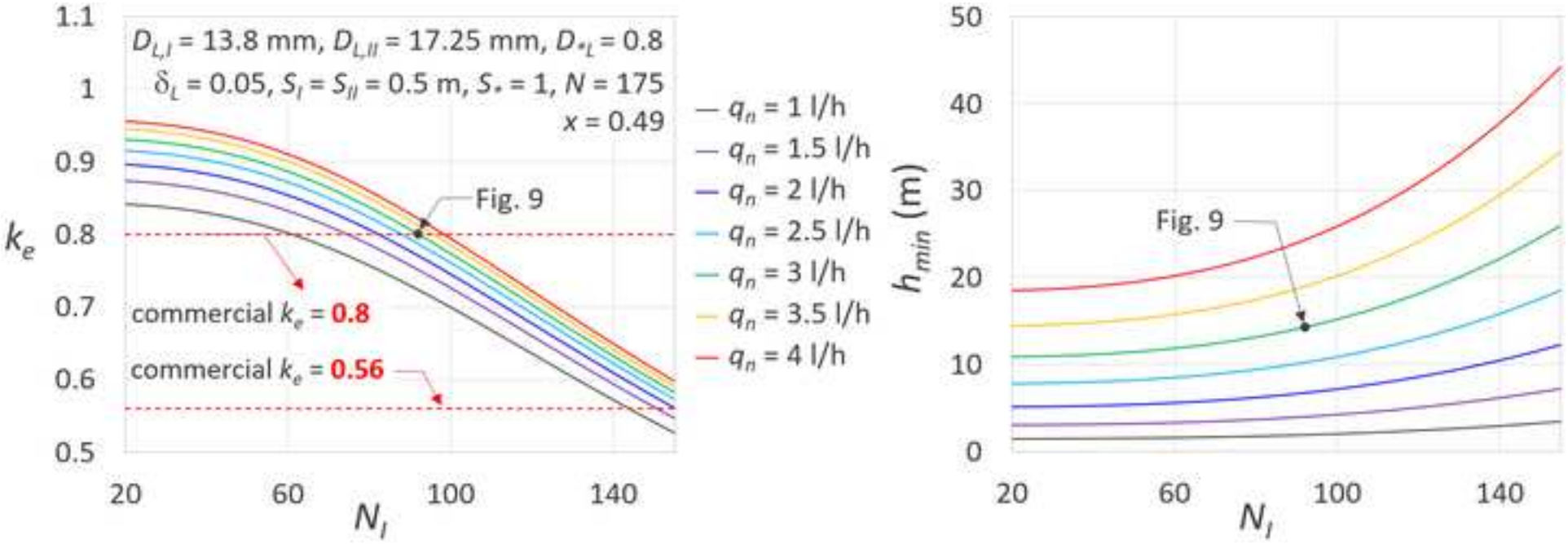

Figure_4ab_REV1

Click here to access/download;Figure;Figure_4ab_REV1.tif

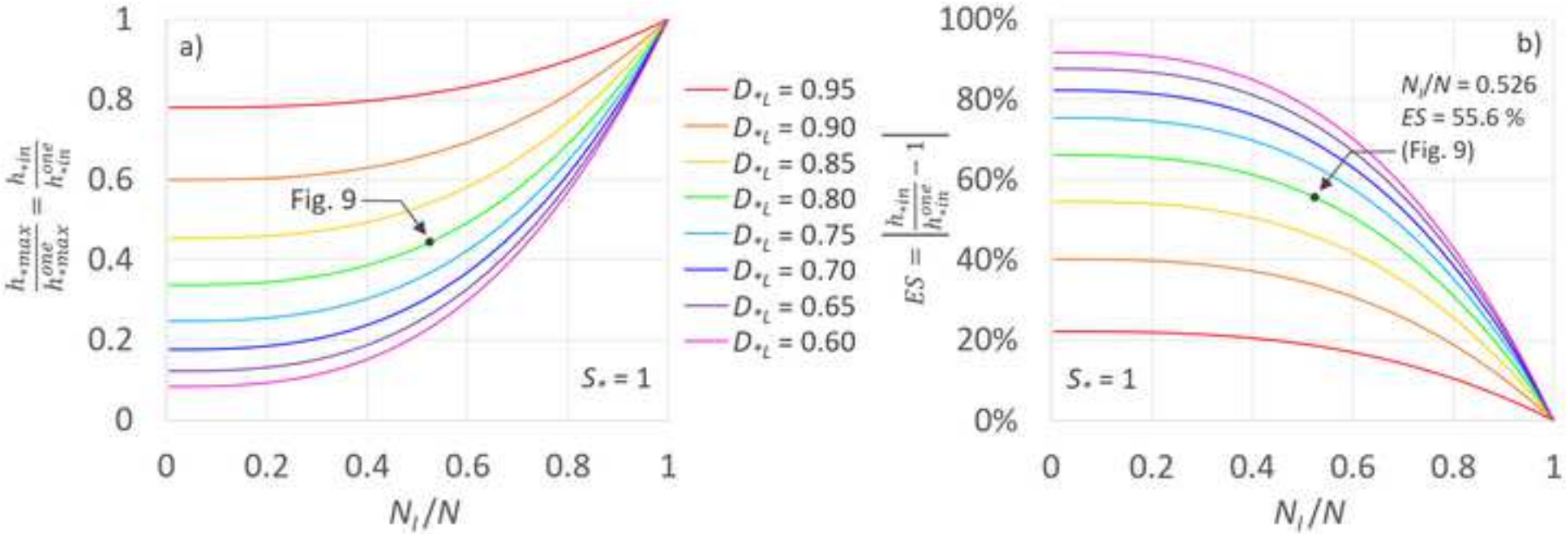

Figure_5

Click here to access/download;Figure;Figure_5.tif

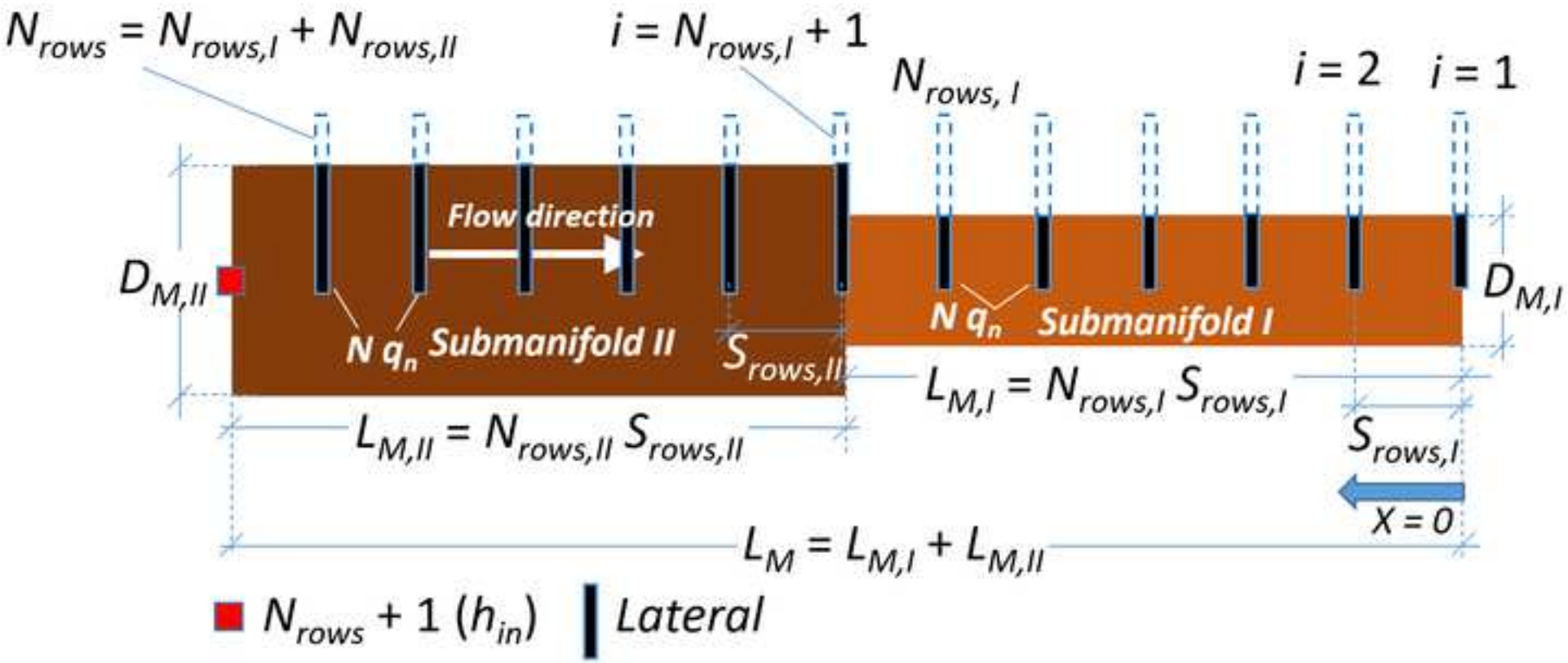

Figure_6ab

Click here to access/download;Figure;Figure_6ab.tif

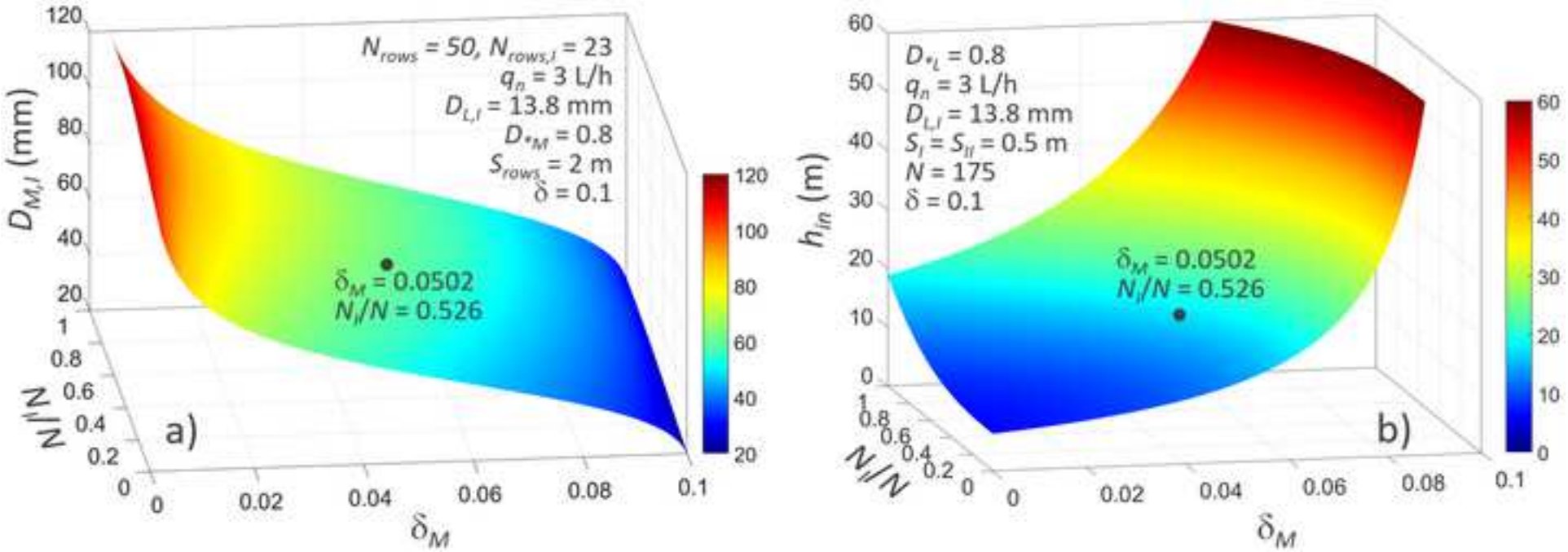

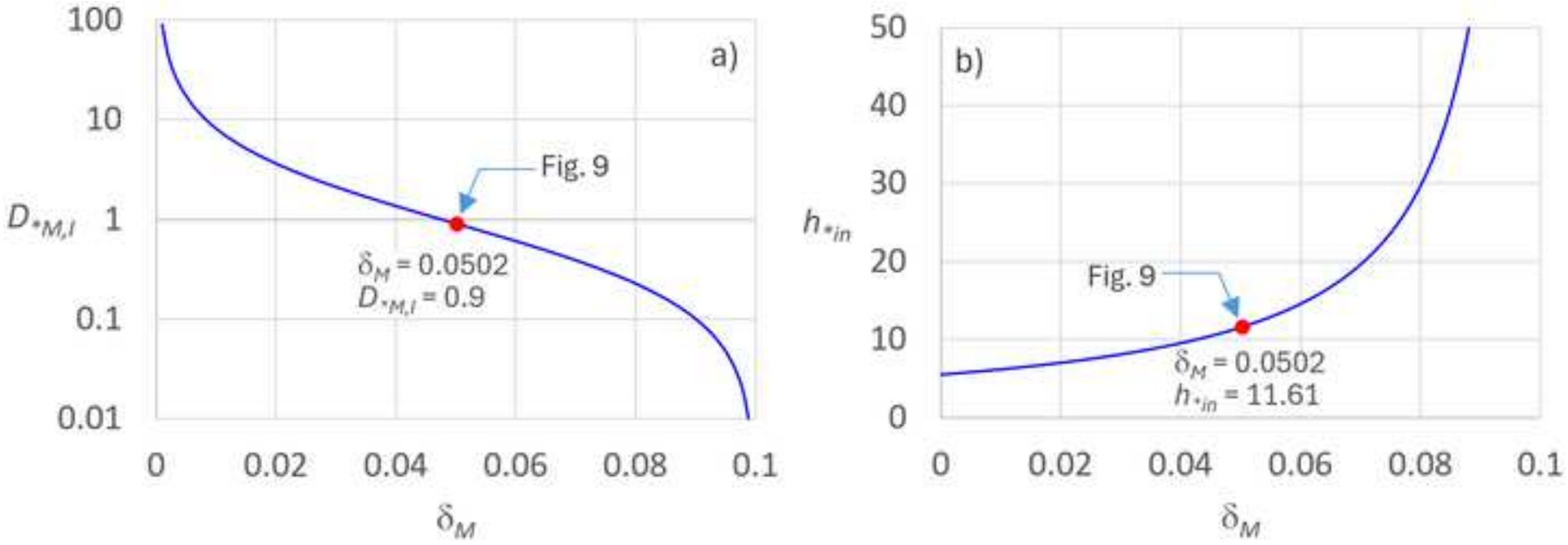

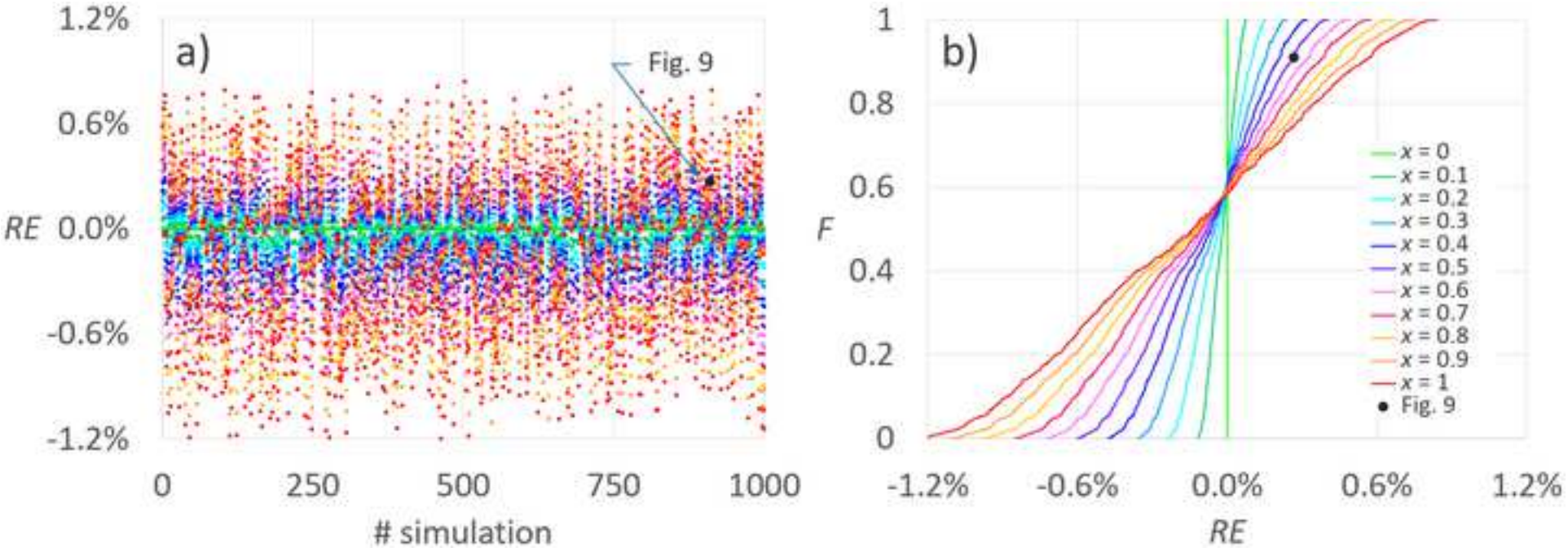

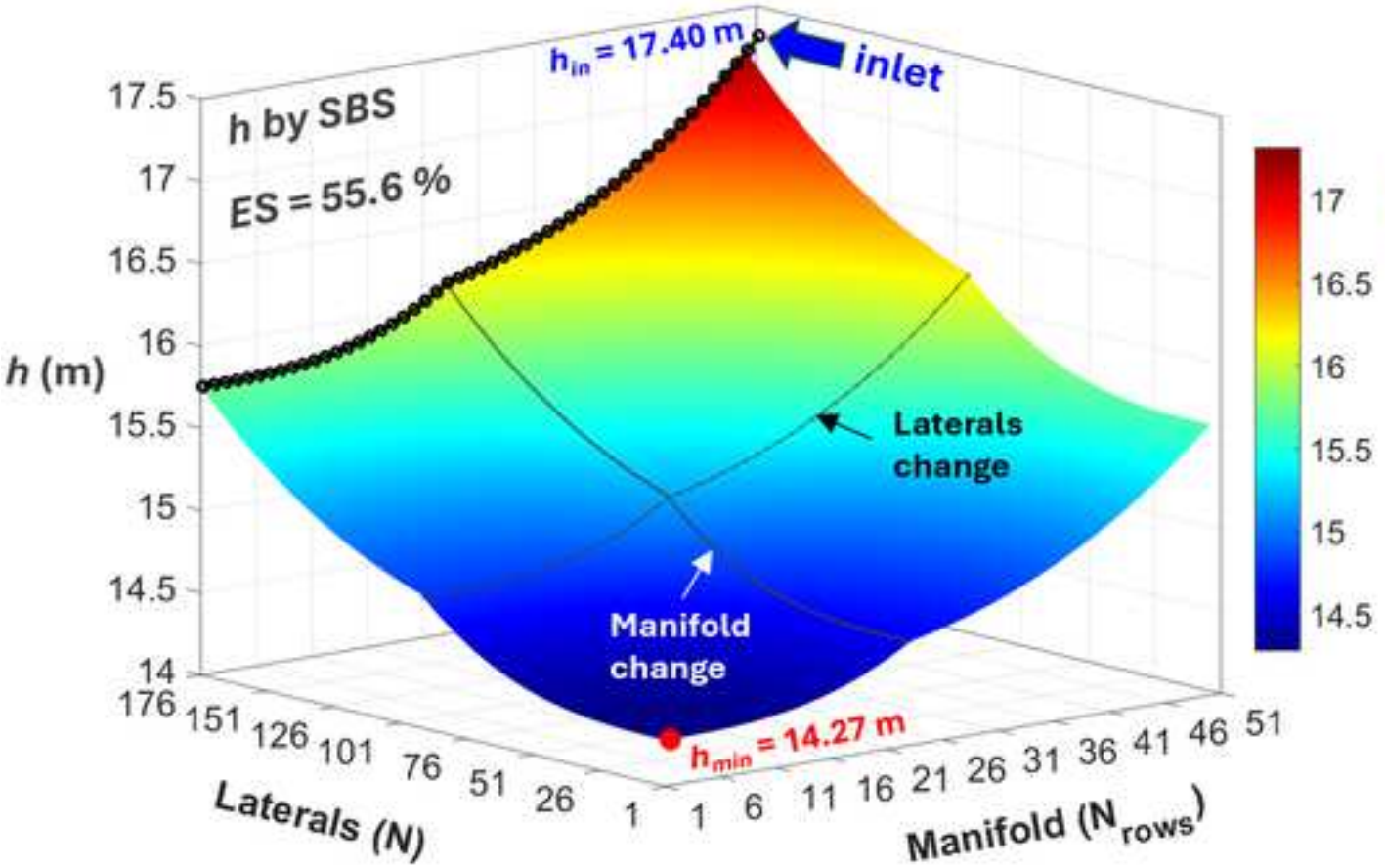

TAPERED LATERALS

S	= 0.5 m
$D_{L,I}$	= 13.8 mm
$D_{L,II}$	= 17.25 mm
k_e	= 0.8 L h^{-1} m^{-x}
x	= 0.49
N_I	= 92
N_{II}	= 83
N	= 175
L	= $N S$ = 87.5 m
δ_L	= 0.05

TAPERED MANIFOLD

S_{rows}	= 2 m
$D_{M,I}$	= 60.7 mm
$D_{M,II}$	= 75.9 mm
$N_{rows,I}$	= 23
$N_{rows,II}$	= 27
N_{rows}	= 50
L_M	= N_{rows} S_{rows} = 100 m
δ_M	= 0.05

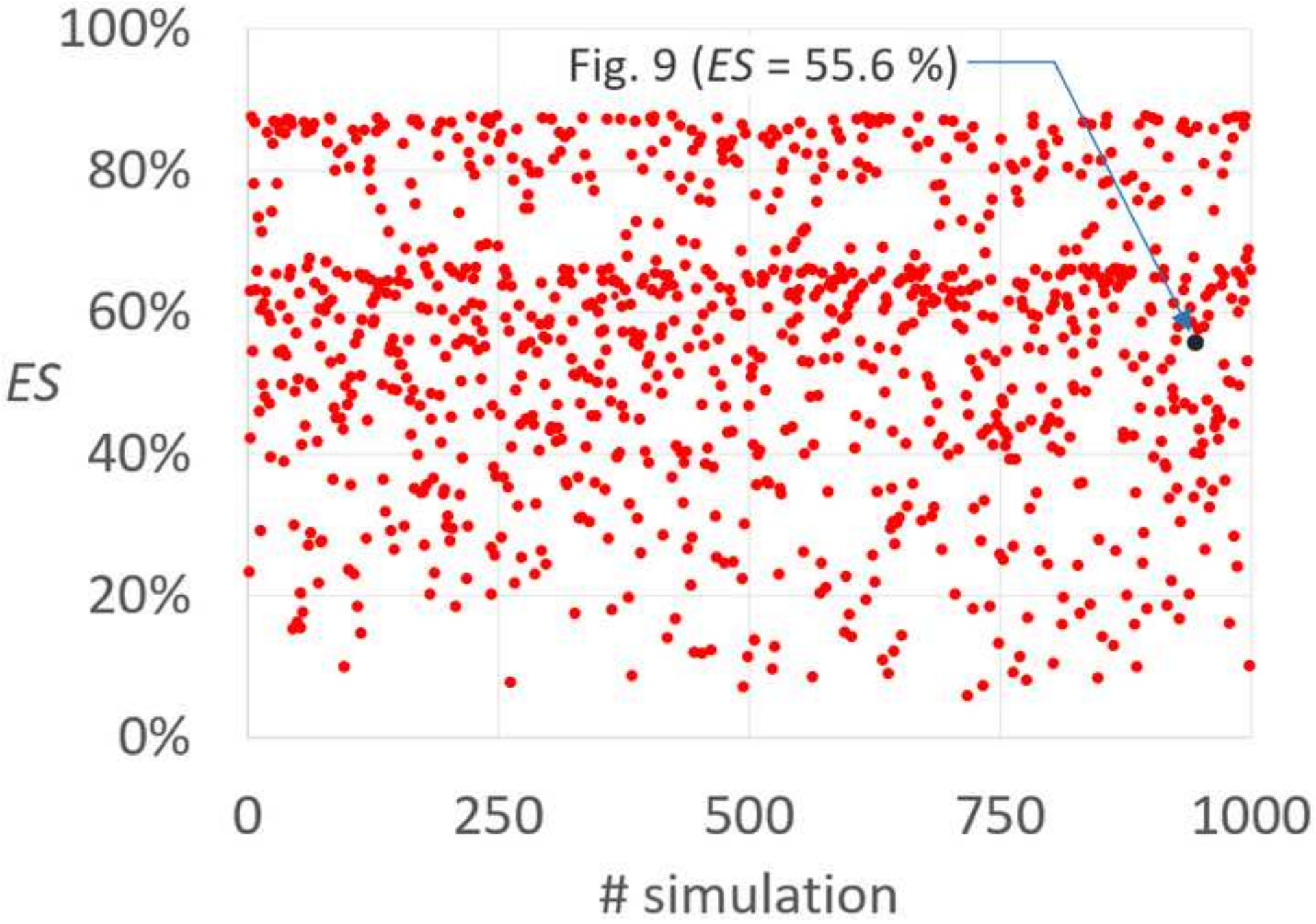

Figure Captions

Fig. 1. Sketch of a horizontal tapered drip irrigation unit.

Fig. 2. Sketch of a horizontal tapered drip lateral.

Fig. 3. For fixed input variables, and x = 0.49, a) k_e coefficient calculated by Eq. (22), and b) corresponding minimum pressure head, h_{min}, versus the number of emitters of the sub-lateral I, N_I, with q_n as a parameter. Horizontal dashed lines refer to k_e values of commercial emitters (Table 1).

Fig. 4. Variation of the h_{*max}/h_{*max}^{one} ratio against N_I/N. Note that $D_{*L} = D_{L,I}/D_{L,II}$ and the black dot refers to the application illustrated in Fig. 9.

Fig. 5. Sketch of a horizontal tapered manifold.

Fig. 6. 3D plot of a) the inside diameter of the sub-manifold I, $D_{M,I}$, determined by Eq. (38), and b) the inlet pressure head, h_{in}, estimated by Eq. (39), versus N_I/N and δ_M. The black dot refers to the h_{in} and $D_{M,I}$ values of the application illustrated in Fig. 9.

Fig. 7. Dimensionless relationships between a) the manifold inside diameter, $D_{*M,I}$ (Eq. 50), and b) the inlet pressure head, h_{*in} (Eq. 51), versus the manifold pressure head tolerance, δ_M. Dots refer to the application illustrated in Fig. 9.

Fig. 8. For # 1000 simulations performed for different random combinations of D, S, k_e, N, q_n, h_{min} and δ, and for different x as a parameter, a) relative error in the inlet pressure head estimation, RE,

calculated by Eq. (52) with respect to that obtained by the exact SBS procedure, and b) corresponding cumulative frequency distributions. Black dot refers to the application illustrated in Fig. 9.

Fig. 9. For the input parameters of the unit designed in line with the suggested procedure, reported on the right panel, the pressure head distribution (PHD), obtained by the SBS method. The drops in pressure heads corresponding to the diameter change along laterals and the manifold can be observed.

Fig. 10. For the #1000 simulations obtained by randomly varying the geometry and hydraulic parameters (Table 2), energy-saving percentage, *ES*, obtained from Eq. (43).